# The integration of angular velocity

Michael Boyle

*Cornell Center for Astrophysics and Planetary Science, Cornell University, Ithaca, New York 14853, USA*

(Dated: May 19, 2017)

A common problem in physics and engineering is determination of the orientation of an object given its angular velocity. When the direction of the angular velocity changes in time, this is a nontrivial problem involving coupled differential equations. Several possible approaches are examined, along with various improvements over previous efforts. These are then evaluated numerically by comparison to a complicated but analytically known rotation that is motivated by the important astrophysical problem of precessing black-hole binaries. It is shown that a straightforward solution directly using quaternions is most efficient and accurate, and that the norm of the quaternion is irrelevant. Integration of the generator of the rotation can also be made roughly as efficient as integration of the rotation. Both methods will typically be twice as efficient naive vector- or matrix-based methods. Implementation by means of standard general-purpose numerical integrators is stable and efficient, so that such problems can be readily solved as part of a larger system of differential equations. Possible generalization to integration in other Lie groups is also discussed.

## I. INTRODUCTION

In the study of kinematics, we sometimes know the angular velocity of an object without knowing the actual orientation of that object. The angular velocity may be known from analysis of torques in dynamical problems, or from data output by instruments in engineering applications. When the object is rotating in some complicated way, finding the orientation from the angular velocity can be difficult; it is neither conceptually obvious, nor computationally trivial. This paper presents several approaches that can be used to find the orientation from a knowledge of the angular velocity.

Problems of this type arise in various situations. In physics, we may be able to calculate the torque exerted on an object by fluid drag, gravitational or electrodynamics effects, or any of various forces. If the moment-of-inertia tensor is known, the angular acceleration may be calculated, from which a trivial integration will provide the angular velocity. The final step of deriving the orientation from the angular velocity is less trivial. Of course, this may be just one part of a much more complicated whole, so that we end up with a coupled system of differential equations, which must be solved simultaneously.

The motivating example for this paper falls into the latter category. The system is an astrophysical binary consisting of a pair of compact objects such as neutron stars or black holes. As the compact objects orbit each other, they give off energy in the form of gravitational waves and spiral in toward one another until they merge in one last enormous burst of energy. But the orbital dynamics can be quite complicated. The recent direct detection of gravitational waves [1] generated by a binary black-hole system has introduced a new era in astronomy. To capitalize on this new window onto the universe, we need to be able to analyze the dynamics of these systems very precisely and with maximum efficiency. In particular, when the black holes have significant spin angular momenta misaligned with their orbital angular momentum, the binary will undergo complicated precession and nutation as it orbits, which directly affects the gravitational-wave signals given off. The underlying purpose of this paper is to enable accurate and efficient modeling of precessing binaries.

But the applicability of this problem ranges far beyond gravitational-wave astronomy. The same mathematics find application in mundane settings for engineering. For example, the micromechanical "gyroscopes" ubiquitous in smartphones and other consumer electronics provide the device's angular acceleration, but cannot provide the instantaneous orientation due to low-frequency noise.[1] The angular velocity must therefore be integrated to arrive at the orientation. Though the principle may be the same, the noise and discrete nature of the angular velocity suggest that low-order methods would be preferable for these devices. This, of course, is a particular example in the broader field of strapdown inertial navigation systems [2–5]. In a completely different setting, Simo [6] pointed out that uniform beams undergoing twisting and bending obey equations formally identical to those for angular velocity, where time is replaced by arc length along the beam and the angular velocity is replaced by the rate of twisting per unit length. This particular problem has even been analyzed using the methods of geometric algebra. Such problems have been analyzed previously in the literature [2–5, 7–10], but those approaches are designed very specifically for pure rotational (and possibly translational) problems without any other evolved quantities, and are frequently tailored even further to approximate particular subclasses of motion. They are therefore not suitable when high accuracy is needed for long integrations involving complicated rotations and other coupled quantities evolving with multiple timescales. In particular, much additional work would be needed to develop adaptive integrators based on these methods, and to incorporate them into general-purpose integrators.

More broadly, techniques for integration in general Lie

---

[1] Such an object is not a gyroscope in the traditional sense of the word, in that it has no spinning member. Rather, it has what is essentially a spring-mounted inertial mass, and changes in the relative orientation of this mass are measured. The coupling between the inertial mass and the surrounding device accounts for the loss of information at low frequencies.

groups have been suggested by various authors, including Magnus [11, 12] and Munthe-Kaas [12, 13], who modified the equations to evolve slightly different quantities so that the solution would remain within the Lie manifold. These approaches are also discussed in Sec. V, in comparison to one of the approaches used in this paper. On a more practical level, numerical integration schemes have been proposed specifically for Lie groups. Crouch and Grossman [12, 14] suggested replacing the additive update method of standard numerical integration schemes with a multiplicative method more suited to Lie groups. Those general techniques have evidently filtered back down to influence the more theoretical approaches to problems involving the familiar simple Lie groups. Bottasso and Borri [15] developed an algorithm that appears to be essentially the Crouch-Grossman technique specialized to the rotation group, while simultaneously treating displacements. Numerous groups have devised other specialized low-order numerical algorithms for such integrations [16–20], as well as several adapted to closely related problems in Lagrangian and Hamiltonian dynamics [21–23]. Candy and Lasenby [24] outlined integrations of rotations using quaternions, and simultaneous treatment of rotations and translations using their natural generalizations in the conformal representation of three-geometry. Two studies compared several of these approaches using simple example rotations—one by Johnson, Williams, and Cook [25]; the other by Zupan and Saje [26]. Unfortunately, both focused on low-order integration methods and achieved very large errors. More recently, Zupan and Zupan [27] and Treven and Saje [28] refined the earlier techniques to achieve much improved stability and accuracy. However, the goal of those works was to find integrators specialized to the problem of rotation. Even in these more theoretical studies, integration of angular velocity has apparently not been successfully tested using general-purpose adaptive numerical integrators and physically motivated rotational examples with coupled variables.

<The preceding shows that there are numerous possible ways of integrating angular velocity—some being fairly subtle variations of others. Of course, in numerical analysis, minor differences can have enormous effects on accuracy and efficiency. For this paper, however, we will not be particularly concerned with finer details of the numerical integrators. The reason for this is twofold. First, many systems involve integration of the angular velocity as just one part of a much large set of equations, other members of which may not be treatable with specialized methods, leaving us wanting to apply a general-purpose integration routine. In fact, we will find that two such routines are capable of very accurate and efficient integration. Second, and more importantly, substantial insight can be gained simply by considering the more basic issue of exactly which set of equations should be solved. General considerations along these lines will suggest the optimal quantities to be evolved.

When integrating angular velocity, the orientation we wish to calculate is defined as a vector basis that is fixed in the rotating system. We call this the "body" frame—though there may not be a clearly defined body involved, as in the case of compact binaries. The body frame is defined with respect to an "inertial" frame that is fixed in space. The most obvious way to define the orientation, then, is to simply express the body frame in the basis of the inertial frame or vice versa. Equivalently, we can define the orientation as the rotation needed to transform the inertial frame into the body frame. Given the wide variety of ways that have been invented to describe rotations, there are similarly many ways to integrate the angular velocity to find the orientation.

Three possible methods for integrating angular velocity will be examined in the following. First is direct integration of the basis vectors of the rotating frame, presented in Sec. II. This is precisely equivalent to integration of the rotation matrix if three orthonormal basis vectors are used. We can, however, improve the accuracy and efficiency of this system by integrating just two of the basis vectors. Of course, this incorporates redundant information, which can—in principle—be removed by constraint damping. It turns out, however, that constraint damping simply stiffens the system, making it far less efficient to integrate. In any case, it appears that the vector approach will always be slower than the alternatives.

The second method examined will use the quaternion representing the rotation, or "rotor", which can be obtained directly as described in Sec. III. There is one additional degree of freedom in this representation, which can be considered the freedom to renormalize the four components. However, this freedom can easily be made redundant simply by applying the quaternion in such a way that the normalization cancels out; as long as the norm is nonzero, it is irrelevant and there are effectively only three degrees of freedom in the rotation represented by the quaternion.

Finally, we can also integrate the *generator* of the rotation, which inherently has just three degrees of freedom. Using quaternion methods again, this can be done without resorting to matrices and their cumbersome methods of exponentiation. There are reasons to expect that generators could provide the most accurate and efficient integration. It turns out that a naive implementation will actually be slower than even the vector implementation because the generator is sometimes very sensitive to the rotation, so that it will change very sharply. This rapid behavior will force the integrator to take smaller steps, slowing the integration considerably. However, we can impose a simple algebraic condition on the generator that avoids those sharp features, making the generator approach robust, and efficient enough to be competitive with even the rotor implementation. The derivation of this approach given in Sec. IV will be more general than strictly necessary because the technique may be interesting for application to integration in other Lie groups, as discussed in Sec. V.

In Sec. VI these methods are then applied to the problem that motivated this paper. We first construct a framework that can be used to devise very complicated rotations that can nonetheless be expressed, along with their time derivatives, in closed form. It is then shown how this can be used to evaluate the accuracy of the integration methods, including the definition of a useful and complete measure of the error.

This framework is then applied to construct a frame undergoing motion that corresponds very closely to the motion experienced by a precessing black-hole binary. This system simply mimics several features of the binary—including fast rotation about a main axis, slower precession around a gradually widening precession cone, and small but fast nutation—but is given by an analytical rotation formula, so that we can compare the numerical results to the exact solution. The particular rates of these rotations are chosen to approximate the equivalent rates in a binary that is very close to merger (the most dynamical stage of the binary's life). But the integration is carried out substantially longer than is required by gravitational-wave data analysis, to provide a more stringent test. The result is excellent performance by the rotor method and by the modified generator method, each approaching the limits of numerical precision. The vector method is roughly twice as slow, and it is argued that this will be a very common feature, so that we can ignore the vector approach, along with the associated matrix approach.

While the simulated binary is a very particular example, it is also a very rigorous one, incorporating large fast motions along with smaller and slower motions. This suggests that we should expect these results to apply much more generally to other rotating systems. Indeed, several very different (though less realistic) additional examples shown in the Appendix bear out these conclusions. In particular, while the generator method is certainly competitive, the rotor method is likely to be slightly more efficient in many cases and possibly more robust. Thus, we can propose the rotor method as the general choice for integrating rotations in three dimensions, while the reasonable effectiveness of the generator suggests that it may be a useful approach in more general Lie groups.

## II. INTEGRATION OF FRAME VECTORS

Perhaps the most obvious approach to integrating the angular velocity to arrive at a frame consists of simply integrating the frame vectors. Assume the rotating system has a set of frame vectors $f_i$, which are stationary in the rotating system. By definition of the angular velocity, with respect to the inertial system we have

$$\frac{\mathrm{d}f_i}{\mathrm{d}t} = \omega \times f_i. \tag{1}$$

If the vectors $f_i$ are unit vectors corresponding to the $x$, $y$, and $z$ directions, this is precisely equivalent to integrating the rotation matrix.

However, there is clearly some redundancy in this naive approach, because we are integrating nine variables representing the three components of each of these three vectors; on the other hand we know that a rotation is determined by just three parameters. Our naive description is redundant because the equations ignore the fact that the frame vectors have unit magnitude, and ignore their mutual orthogonality. We can reduce the redundancy by eliminating one of the vectors: evolve only two of the vectors (say $f_0$ and $f_1$), and deduce the third by taking their cross product ($f_2 = f_0 \times f_1$). It would be possible to

remove further degrees of freedom, for example by computing only two of the components of $f_0$, and computing the third using the normalization of the vector. But this would leave it determined only up to a sign, so we would need additional logic to choose that sign. The additional complications are likely not worth the trouble.

During a numerical integration, any violation of the constraints due to finite precision could grow. In that case, there are additional methods of enforcing constraints—the standard methods being damping and projection [12]. Constraint projection involves simply replacing the solution after each time step with the nearest solution that satisfies the constraints. In this case, one could use a standard Gram-Schmidt orthonormalization procedure. Constraint damping involves the addition of terms to the differential equations that drive the solution back toward the constraint surface. For example, to enforce the constraint that elements of our frame have unit norm, we could modify the equation above to read

$$\frac{\mathrm{d}f_i}{\mathrm{d}t} = \omega \times f_i + \lambda_i (1 - f_i \cdot f_i) \, f_i, \tag{2}$$

where $\lambda_i$ is some constant that sets the timescale on which constraint violations are damped as $1/\lambda_i$. When the norm of the vector is 1, this does not modify the evolution in any way; when it is different, this simply forces the vector back to the nearest constrained value. It must be noted, however, that this makes the equations stiff, which typically results in less efficient integration. We could also add terms to damp violations of the orthogonality constraint, as in

$$\frac{\mathrm{d}f_1}{\mathrm{d}t} = \omega \times f_1 + \mu \left( \frac{f_0 \times (f_1 \times f_0)}{|f_0 \times (f_1 \times f_0)|} - f_1 \right), \tag{3}$$

for some constant $\mu$. When $f_1$ has unit norm and is orthogonal to $f_0$, the terms in parentheses cancel out, so there is no change in the evolution; otherwise, that factor drives $f_1$ toward perpendicularity in the $f_0$-$f_1$ plane. Again, however, these elaborate alterations can be expected to increase the complexity and decrease the robustness of the solution, so it is not clear how useful they can be.

## III. INTEGRATION OF ROTORS

Though integration of the frame vectors presents a very clear and effective way of integrating angular velocity, the redundant information is unappealing from an aesthetic standpoint. Furthermore, in numerical applications, we can expect that the redundancy might reduce the accuracy and efficiency of integration. Thus, it might be preferable to find an alternative method of integrating. Ultimately, we are interested in computing a rotation that corresponds to the given angular velocity, so we might wonder whether it is possible to *directly* find that rotation. That is, we can search for the operator performing the rotation, rather than the vectors being rotated. While rotation matrices are probably the most familiar way of approaching rotations, we noted above that this would be equivalent to

integrating three orthogonal frame vectors, having nine degrees of freedom to represent a three-dimensional problem. A more elegant and modern approach—yet simpler and easier to use, once they are understood—is found in quaternions. Though the early history was tragically muddled by the misguided idea that vectors and quaternions were incompatible [29], they are now seen as two aspects of a more powerful unifying theory: geometric algebra [30, 31], in which both quaternions and the more familiar vector algebra arise as specializations in three dimensions. Because of their advantageous numerical and conceptual properties, quaternions have found successful application in various fields including computer graphics, robotics, molecular dynamics, celestial mechanics, and orbital dynamics [31, 32]. Here, we find that they also give rise to a simple method for integrating angular velocity.

Quaternions have a scalar part and a "vector" part,[2] so that vectors may be considered quaternions with scalar part 0, and quaternions with scalar part 0 may be considered vectors equivalently. At this level, quaternions may be considered precisely four-dimensional vectors. However, there is a crucial additional structure provided with them: they can be multiplied together. The details of this multiplication are available in any standard reference—perhaps the best being Ref. [31]—but two salient features are that it is associative but not commutative. For our purposes, the most interesting application of multiplication is the rotation of a vector. Given a vector $v$ and a nonzero quaternion $R$, we can construct a new vector[3]

$$v' = R\,v\,R^{-1}.\qquad(4)$$

It turns out that $v'$ is simply the rotation of $v$ about the axis given by the vector part of $R$, and the angle of that rotation is related to the ratio of the scalar part to the magnitude of the vector part. Because the quaternion effects the rotation of vectors, Clifford named this object a "rotor" [33]. Then, rather than analyzing the evolution of several vectors being rotated, we will analyze the evolution of the single rotor effecting this rotation. It is true that a quaternion has four elements, and hence one more degree of freedom than the space of rotations being modeled; nonetheless, this is a substantial improvement over the six to nine components of the vector/matrix approach.

Before we see how this gives rise to an evolution equation, a brief note is in order. Clifford actually imposed another requirement on what he would call a rotor, which is also usually imposed elsewhere in the literature. That is: a rotor should have unit magnitude, meaning that the sum of the squares of the scalar and vector components should equal 1. Then, rather than Eq. (4), Clifford and others generally use $v' = R\,v\,\bar{R}$, where $\bar{R}$ is the conjugate which simply reverses the sign of the vector part of $R$. When the magnitude is 1, these are precisely equivalent. However, due to numerical error, this constraint may be violated.[4] If we were to use the conjugate instead of the inverse, $v'$ would have a different magnitude than $v$, and so would no longer be a rotation. Using the inverse instead makes the magnitude irrelevant—as long as it is nonzero so that an inverse actually exists. We are abusing language slightly in calling these objects rotors (the more standard term being "spinors"), but the intent is really identical.

Now, to derive an evolution equation, we assume that $v$ is some constant vector, perhaps representing an initial value, while $v'(t)$ is evolving in the inertial frame. This will correspond via Eq. (4) to some rotor $R(t)$, whose evolution we will now relate to $\omega$ (dropping the arguments $t$ for simplicity). First, we can use the product rule to differentiate $R\,R^{-1} = 1$ and find

$$\frac{d}{dt}R^{-1} = -R^{-1}\frac{dR}{dt}R^{-1}.\qquad(5)$$

Using this result, it is not hard to show that

$$\frac{dv'}{dt} = \frac{d}{dt}\left(R\,v\,R^{-1}\right) = \left[\frac{dR}{dt}R^{-1}, v'\right],\qquad(6)$$

where the brackets in the last expression denote the usual commutator. Similar calculations show that the term $\frac{dR}{dt}R^{-1}$ is a pure vector if and only if the quantity $R\,\bar{R}$ is constant in time (though it need not equal 1). In that case, a simple exercise using the definition of quaternion multiplication shows that we can rewrite this last expression as

$$\frac{dv'}{dt} = \left(2\frac{dR}{dt}R^{-1}\right)\times v',\qquad(7)$$

where the symbol $\times$ is just the usual vector cross product. Now, recalling the standard angular-velocity formula

$$\frac{dv'}{dt} = \omega \times v',\qquad(8)$$

and noting that these results hold for arbitrary $v$, we see that

$$\omega = 2\frac{dR}{dt}R^{-1}.\qquad(9)$$

---

[2] In fact, geometric algebra makes clear that the "vector" part would be more coherently called a "bivector" part [31], where rather than a vector representing the axis of a rotation the bivector represents the plane in which the rotation takes place. This generalizes perfectly to vector spaces of any dimension and signature. Coincidentally, a bivector in three dimensions has three components, just like a vector. Misunderstanding of this accidental equality was the origin of the acrimonious debate between vector partisans and quaternion partisans in the late nineteenth century [29]. Even in three dimensions clarifying the distinction can lead to deeper understanding of the geometry, but we will use more standard terminology in this paper.

[3] For numerical applications, rather than using quaternion multiplication directly, it is roughly twice as efficient to implement this equation as $v' = v + 2\,r \times (s\,v + r \times v)/m$. Here $s$ and $r$ are the scalar and vector parts of $R$, and $m$ is the sum of the squares of the components of $R$.

[4] It is also worth noting that there are cases in which the alternative form of Eq. (4) using the conjugate in place of the inverse may be used to describe changes in a vector that should *not* preserve its magnitude, using quaternions that intentionally have non-unit magnitude. For example, the quaternion may be used to model eccentric orbits—in which case the magnitude should change as the orbiting body traces out the ellipse—leading to enormous simplifications [31, 34].

As promised, this relates the rotor $\mathbf{R}$ to the angular velocity $\omega$. In fact, we can turn this into a first-order differential equation:

$$\frac{d\mathbf{R}}{dt} = \frac{1}{2}\omega\,\mathbf{R}. \tag{10}$$

As long as $\omega$ is known as a function of time and possibly of $\mathbf{R}$ (but not of $d\mathbf{R}/dt$), standard theorems on ordinary differential equations apply, which show that given initial data for $\mathbf{R}$, we can simply evolve the four components of this equation to find $\mathbf{R}$ as a function of time.[5]

We will see below that quaternions can be exponentiated readily. One might then expect that Eq. (10) could be integrated using the exponential:

$$\mathbf{R}(t) = \exp\left[\frac{1}{2}\int_0^t \omega(t')\,dt'\right]\mathbf{R}(0). \tag{11}$$

This actually may be a valid solution to the differential equation, but only when $\omega(t_1)$ commutes with $\omega(t_2)$ for any pair of times $t_1$ and $t_2$, and with $\mathbf{R}(0)$—that is, when the rotation all takes place about a single axis. The quaternion exponential is substantially more complicated than the real and complex exponentials, because of the noncommutativity of the quaternion product. More generally, when the direction of $\omega$ varies in time, we do not have commutativity, and we must therefore treat the problem as a coupled system of ordinary differential equations for the four components of $\mathbf{R}(t)$.

One important point to note about our result, Eq. (10), is that we derived it without any constraints. The only assumptions that went into the derivation were differentiability of the various elements, and the existence of an inverse of $\mathbf{R}$—which will be the case as long as $\mathbf{R} \neq 0$. In particular, we did not assume that $\mathbf{R}$ has unit magnitude. Interestingly enough, Eq. (10) results when we use the alternative form of Eq. (4) mentioned above in which unit magnitude is assumed. Thus, we could think of our approach as a form of constraint projection. In fact, the rotation group SO(3) is topologically the same as $\mathbb{R}P^3$, which is usually described as $\mathbb{R}^4$ with the origin removed, subject to identification of all points that are scalar multiples of each other [35]. In a sense, we are evolving in that larger space, and making the identification later. But it is clear that Eq. (10) is the correct evolution equation, *even in the larger space*. Many of the references cited in Sec. I go to great lengths to enforce the unit magnitude of the rotor; the argument here suggests that such effort is wholly unnecessary.

## IV. INTEGRATION OF GENERATORS

The solution given by Eq. (11) suggests another possible approach to integrating angular velocity. The quantity in

the exponential is called the generator of the rotation, and is linear in the angular velocity for this solution. It is true that this solution is not valid for more general angular velocities, in which the direction of the angular velocity changes. But perhaps the general solution may at least be *dominated* by linear behavior, which would suggest useful perturbative expansions and effective numerical implementation. This approach also finds motivation in the formalism of Lie theory. The rotation group is a Lie group, and every Lie group is governed locally by its corresponding Lie algebra; a path through the group is given by integrating the differential motions given by elements of the algebra, in complete generality for *all* Lie groups. The relation between the group and the algebra is given—locally at least—by the exponential function. Thus, in this section, we investigate computing the *generator* of the rotation, rather than the rotation itself. The derivation used here was first introduced in Ref. [36], though the key equation, Eq. (18), was derived much earlier using a very different approach by Grassia [37] and then by Candy and Lasenby [24] using still another approach. The present derivation is more complicated, but has the advantage of generalizing to other Lie groups.

To begin, we relate a rotor $\mathbf{R}$ to its generator $\mathbf{r}$ by $\mathbf{R} = e^{\mathbf{r}}$. Here the generator $\mathbf{r}$ is a quaternion with zero scalar part, which is sometimes called a pure vector, and exponentiation is given by the usual series expression incorporating integer powers of the generator. For rotations, this vector $\mathbf{r}$ has the interpretation of being the axis about which the rotation takes place, and its magnitude is half the angle of that rotation. In any case, Lie theory then provides us with a formula [38] for the derivative of $\mathbf{R}$ in terms of $\mathbf{r}$ and its derivative:

$$\frac{d\mathbf{R}}{dt} = \frac{de^{\mathbf{r}}}{dt} = \int_0^1 e^{s\mathbf{r}}\frac{d\mathbf{r}}{dt}e^{(1-s)\mathbf{r}}\,ds. \tag{12}$$

Multiplying this equation on the right by $\mathbf{R}^{-1} = e^{-\mathbf{r}}$, it is clear that we will obtain a formula relating the angular velocity (9) to the generator of the rotation and its time-derivative. To put this into a more useful form, however, we need to evaluate the integral and simplify.

We can write a standard formula [39] as

$$e^{\mathbf{p}}\,\mathbf{q}\,e^{-\mathbf{p}} = \sum_{k=0}^{\infty}\frac{1}{k!}\,\mathrm{ad}_{\mathbf{p}}^k\,\mathbf{q}, \tag{13}$$

where the adjoint function is defined recursively by

$$\mathrm{ad}_{\mathbf{p}}^0\,\mathbf{q} = \mathbf{q}, \tag{14a}$$

$$\mathrm{ad}_{\mathbf{p}}^1\,\mathbf{q} = [\mathbf{p}, \mathbf{q}], \tag{14b}$$

$$\mathrm{ad}_{\mathbf{p}}^{k+1}\,\mathbf{q} = \left[\mathbf{p}, \mathrm{ad}_{\mathbf{p}}^k\,\mathbf{q}\right], \tag{14c}$$

and $[\boldsymbol{a}, \boldsymbol{b}] = \boldsymbol{ab} - \boldsymbol{ba}$ represents the Lie bracket. We now have

$$\omega = 2\frac{d\mathbf{R}}{dt}\,\mathbf{R}^{-1} = 2\int_0^1\sum_{k=0}^{\infty}\frac{1}{k!}\,\mathrm{ad}_{s\mathbf{r}}^k\,\frac{d\mathbf{r}}{dt}\,ds. \tag{15}$$

Formally, at least, this fulfills our objective of relating $d\mathbf{r}/dt$ to $\omega$ and $\mathbf{r}$. It should be noted that, up to this point, the derivation

---

[5] If we simply *assume* that $\mathbf{R}$ obeys an equation of the form (10), for a general quaternion $s + \omega$ with scalar part $s$, then $d(\mathbf{R}\bar{\mathbf{R}})/dt = s\,\mathbf{R}\,\bar{\mathbf{R}}/2$. But since we impose Eq. (10) with $s = 0$, we know that $\mathbf{R}\,\bar{\mathbf{R}}$ is constant in time. This shows that the conversion of Eq. (6) into Eq. (7) is, at least, consistent.

has been completely general[6] and applies to any Lie algebra. This will be discussed further in Sec. V.

We can now specialize to $\mathfrak{so}(3)$, and use induction to prove

$$\mathrm{ad}_{\mathbf{p}}^k \, \mathbf{q} = \begin{cases} \mathbf{q} & k = 0; \\ (-1)^{(k-1)/2} \, [\mathbf{p}, \mathbf{q}] \, (2\,\mathrm{p})^{k-1} & k > 0 \text{ odd}; \\ (-1)^{(k-2)/2} \, [\mathbf{p}, [\mathbf{p}, \mathbf{q}]] \, (2\,\mathrm{p})^{k-2} & k > 0 \text{ even}. \end{cases} \quad (16)$$

Plugging this expression into Eq. (15), evaluating the sum, and integrating, we find

$$\omega = 2\,\dot{\mathbf{r}} + \frac{\sin^2 \mathrm{r}}{\mathrm{r}^2}\Big[\mathbf{r}, \dot{\mathbf{r}}\Big] + \frac{\mathrm{r} - \sin \mathrm{r} \cos \mathrm{r}}{2\mathrm{r}^3}\Big[\mathbf{r}, \big[\mathbf{r}, \dot{\mathbf{r}}\big]\Big]. \quad (17)$$

For $\mathrm{r} = \pi$, we have $\mathbf{r} = -1$, and so this reduces to $\dot{\mathbf{r}} = \omega/2$. For smaller values of r, we can solve this equation for $\dot{\mathbf{r}}$. Using the fact that in three dimensions, $[a, b] = 2\,a \times b$ (with $\times$ representing the usual vector cross product), we can write the solution as

$$\dot{\mathbf{r}} = \frac{1}{2}\omega \times \mathbf{r} + \omega\,\frac{\mathrm{r}\cot \mathrm{r}}{2} + \mathbf{r}\,\frac{\mathbf{r} \cdot \omega}{2\,\mathrm{r}^2}(1 - \mathrm{r}\cot \mathrm{r}). \quad (18)$$

This differential equation for $\mathbf{r}$ can be used to integrate the orientation of the system given $\omega$ as a function of $t$ and possibly $\mathbf{r}$, and so to find $\mathbf{r}$ as a function of time.

One point to note here is that the magnitude of $\mathbf{r}$ can be unbounded when integrating this equation. In realistic applications, this would happen very rarely, because it requires the rotation to return to the identity rotation. However, if the rotation is restricted to a fixed axis, or if there is some other reason the system should happen to return to the identity, this can occur. And it can cause problems in numerical integrations when the system returns *approximately* to the identity. At these times, the integration becomes very delicate, requiring high precision to retain accuracy in the result. We can avoid this condition, however, using the fact that different values of the generator represent the same rotation. In particular,

$$\exp[\mathbf{r}] \quad \text{and} \quad \exp\Big[\mathbf{r} + n\,\pi\frac{\mathbf{r}}{\mathrm{r}}\Big] \quad (19)$$

represent identical rotations for any integer $n$.[7] Thus, whenever $\mathrm{r} \geq \pi/2$, we can reset the value of the generator according to

$$\mathbf{r} \rightarrow \mathbf{r} - \pi\frac{\mathbf{r}}{\mathrm{r}}. \quad (20)$$

————

[6] We assumed that it is always possible to find a generator satisfying $\mathbf{R} = e^{\mathbf{r}}$ because the rotation group is connected, although we will see below that such a generator is not unique. For more general Lie groups, only an element in the connected component of the identity can be written in this way, but arbitrary elements may be written as the product of such an exponential and some (componentwise-constant) element in the connected component of the result: $\mathbf{R} = e^{\mathbf{r}} \mathbf{R}_0$. The derivation of Eq. (15) follows in exactly the same way.

[7] This is a generalization to quaternions of the more familiar result from complex algebra $e^z = (-1)^n e^{z + \pi i n}$. The negative sign is irrelevant for our purposes because the rotor is used twice to rotate a vector, so the sign drops out.

When $\mathrm{r} = \pi/2$, this transformation is simply $\mathbf{r} \rightarrow -\mathbf{r}$. This means that rather than rotating through $\pi$ about the given axis, we rotate by $\pi$ about the axis in the opposite sense—which is an equivalent rotation. For $\mathrm{r} > \pi/2$ this reduces the magnitude of the generator below $\pi/2$. But in either case the derivative now changes so that, rather than increasing back toward $\pi/2$, the magnitude begins to decrease. We will find below that this is a crucial step in making integration of angular velocity by generators an efficient approach.

## V. INTEGRATION IN GENERAL LIE GROUPS

Though not directly related to the purpose of this paper, the previous section may be useful in very different situations, which we now take a brief detour to discuss. As noted below Eq. (15), the derivation of that expression was entirely general, and applies to any Lie group. The resulting approach to integration is very similar in motivation to algorithms described by Magnus [11, 12] and Munthe-Kaas [12, 13] for integration in Lie groups. However, both assumed that expressions comparable to the sum in Eq. (15) could not be calculated explicitly, and would need to be truncated at some finite term instead. Higher powers of the adjoint simplify in our case using properties of $\mathfrak{so}(3)$, which results in a recursive expression that can be summed explicitly, avoiding truncation.

For more general Lie groups, we can expect a similar simplification whenever there exists some $K$ such that for all $\mathbf{p}$ and $\mathbf{q}$, $\mathrm{ad}_{\mathbf{p}}^K \, \mathbf{q}$ can be written as a linear combination of the $\mathrm{ad}_{\mathbf{p}}^k \, \mathbf{q}$ with $k < K$. This will always be true for nilpotent algebras; indeed, for nilpotent algebras there exists a $K$ such that $\mathrm{ad}_{\mathbf{p}}^K \, \mathbf{q} = 0$, which leaves us with a summation over a finite series of terms. However, ours is a much weaker condition than nilpotency, and so will be true for a more general class of Lie groups.

Other important problems for which such a simplification occurs include those for which the evolution remains confined to a three-dimensional subspace. To see how, we need to use the form of the Lie bracket as given by an antisymmetrized product between two vectors: $[a, b] = a\,b - b\,a$. In general, the products on the right-hand side of this expression need not be defined; a Lie algebra only requires a definition of the bracket. However, there is a construction called the universal enveloping algebra [40], whereby every Lie algebra can be expressed as a subspace of an associative algebra in which such products *are* defined. We can simply regard the original algebra as being embedded within the enveloping algebra—and thus use the same symbols for notational simplicity. Using the associative product from the enveloping algebra, we have quite generally[8]

$$\mathrm{ad}_{\mathbf{p}}^k \, \mathbf{q} = \sum_{j=0}^{k} (-1)^{j+k} \binom{k}{j} \mathbf{p}^j \, \mathbf{q} \, \mathbf{p}^{k-j}. \quad (21)$$

————

[8] Again, this is proven using a simple induction, along with the definition of the adjoint, Eqs. (14).

Whenever $\mathbf{p}^\ell$ is a scalar for some $\ell < k$, we can pull such a factor out of the terms in this sum. Then $\mathrm{ad}_{\mathbf{p}}^k \mathbf{q}$ can be written as a linear combination of $\mathrm{ad}_{\mathbf{p}}^{k-\ell} \mathbf{q}$ and lower-order terms. Because the adjoint is defined recursively, all higher-order terms will similarly collapse, so that the sum in Eq. (17) can be written using only a finite number of adjoints. It may be useful to consider these statements applied to the case of $\mathfrak{so}(3)$, using quaternions. The generator $\mathbf{p}$ is a "pure vector" quaternion, and we know that $\mathbf{p}\,\mathbf{p}$ is always a scalar. So we have $\ell = 2$, which means that we know $\mathrm{ad}_{\mathbf{p}}^3 \mathbf{q}$ is a scalar multiple of $\mathrm{ad}_{\mathbf{p}}^1 \mathbf{q}$, and so on. This is how Eq. (16) can be so simple.

Doran *et al.* [41] presented a particularly useful formulation in which the universal enveloping algebra is a bivector algebra—a subalgebra of a Clifford algebra, also known as a geometric algebra. The associative product is the Clifford product. It is also known [30, 31] that any bivector in a space of three dimensions or fewer may be written as a blade—the Clifford product of two anticommuting vectors. Let us write $\mathbf{p} = v\,w$ for some vectors $v$ and $w$. Then we have $\mathbf{p}\,\mathbf{p} = v\,w\,v\,w = -v\,v\,w\,w$. In any Clifford algebra, the product of a vector with itself is a scalar, by definition, so the last expression is a scalar. Thus, for any problem in which the generators are restricted to a three-dimensional subspace, we will always obtain Eq. (16), which will always result in an expression like Eq. (17)—with an appropriately generalized definition of the angular velocity, and the sine and cosine possibly replaced by their hyperbolic counterparts. Slightly more generally, we do not need $\mathbf{p}^\ell$ to be a *scalar*, but our result is obtained as long as that term commutes with the lower-order adjoints. In Clifford algebra, such conditions will frequently occur, for example, when $\mathbf{p}^\ell$ is a scalar plus pseudoscalar (a generalized complex number), which will always commute with a bivector.

The bivector presentation of, for example, Doran *et al.* [41] suggests that the number of degrees of freedom for generators in an $n$-dimensional Lie algebra should scale as $\binom{n}{2}$, whereas the equivalent of the rotor presentation of the group should scale as $2^{n-1}$, meaning that integration by generators always reduces the number of equations needed—and the benefit increases rapidly with the dimension of the algebra. The message is simply that we may expect cases in which the problem simplifies, and the sum in Eq. (13) may be evaluated exactly; the need for truncation should not be assumed. But with or without simplification, integration by generators may provide an accurate and efficient approach to integrating within general Lie groups.

## VI. NUMERICAL EXAMPLE

To evaluate the methods presented in Secs. II, III, and IV, we need a problem that is adequately complicated to provide a realistic challenge, yet also simple enough to obtain an analytical solution for comparison to the numerical results. First, a broad framework for developing this type of problem is presented, along with the appropriate method of measuring the error when different approaches may be taken. Then, because this paper is motivated by the precessing black-hole binary

system, we will construct a problem that emulates the types of rotation and timescales seen in that system. This problem will then be solved numerically and compared to the exact answer as a means of evaluating the various integration methods.

### A. Framework

The discussion around Eq. (11) showed that it is simple to integrate rotation about a fixed axis. It is also a simple matter to differentiate a rotor describing rotation about a fixed axis:

$$\mathbf{R}(t) = \mathrm{e}^{f(t)\,\mathbf{v}} \quad \implies \quad \dot{\mathbf{R}}(t) = \dot{f}(t)\,\mathbf{v}\,\mathbf{R}(t) = \dot{f}(t)\,\mathbf{R}(t)\,\mathbf{v}, \quad (22)$$

for an arbitrary differentiable function $f(t)$ and an arbitrary constant $\mathbf{v}$. However, we also have the product rule

$$\mathbf{R}(t) = \mathbf{R}_1(t)\,\mathbf{R}_2(t) \quad \implies \quad \dot{\mathbf{R}}(t) = \dot{\mathbf{R}}_1(t)\,\mathbf{R}_2(t) + \mathbf{R}_1(t)\,\dot{\mathbf{R}}_2(t).$$
$$(23)$$

This, of course, can be iterated to differentiate arbitrary products of rotors. We also know how to differentiate inverse rotors, by Eq. (5). But we can construct highly nontrivial rotations just be composing them in this way, even when each individual rotation is a rotation about a fixed axis. For example, define

$$\mathbf{R}_1(t) = \mathrm{e}^{f(t)\,\mathbf{v}}, \quad (24\mathrm{a})$$

$$\mathbf{R}_2(t) = \mathrm{e}^{g(t)\,\mathbf{w}}, \quad (24\mathrm{b})$$

$$\mathbf{R}(t) = \mathbf{R}_1(t)\,\mathbf{R}_2(t)\,\mathbf{R}_1^{-1}(t). \quad (24\mathrm{c})$$

Here, $\mathbf{R}(t)$ is a rotation through the angle $2\,g(t)$ about the axis $\mathbf{w}'(t) = \mathbf{R}_1(t)\,\mathbf{w}\,\mathbf{R}_1^{-1}(t)$. That is, the axis of rotation is itself rotated by $\mathbf{R}_1(t)$, so this is now a much more complicated rotation. Yet it is very simple to compute the derivative

$$\dot{\mathbf{R}} = \dot{f}\,\mathbf{v}\,\mathbf{R} + \dot{g}\,\mathbf{R}_1\,\mathbf{R}_2\,\mathbf{w}\,\mathbf{R}_1^{-1} - \dot{f}\,\mathbf{R}\,\mathbf{v}. \quad (24\mathrm{d})$$

It should be noted that $f(t)$ and $g(t)$ can be quite complicated, but as long as their derivatives are given in closed form, the derivative of $\mathbf{R}(t)$ can also be given in closed form. Moreover, we can compose several such rotations to apply different physically motivated effects. Section VI B will show that it is possible to emulate various features of the very complex motion of a precessing black-hole binary using just a few simple rotations which can easily be differentiated analytically.

Now, given an exact rotor function of time and its derivative, we can use Eq. (9) to find its angular velocity. We then apply the methods of the previous sections to integrate that angular velocity, and compare the result to the analytical rotation to evaluate the accuracy and efficiency of our methods. But before we can compare the results, we need to decide on what quantities to compare because the methods give different types of results. The vector method gives a pair of vectors, the rotor method a rotor, and the generator method a generator. We could, for example, exponentiate the result of the generator method to find the corresponding rotor. But then it is not clear how to define the rotor corresponding to a pair of vectors; it is possible, but there is ambiguity that may hide error somehow.

Ultimately, the purpose behind integrating the angular velocity is to be able to relate vectors in the rotating system

to vectors in the inertial system. It is sufficient to work with bases of the inertial and rotating systems, so we can construct an error measure that is both simple—because it deals only with the bases—and captures all possible error. To do so, we define the inertial frame $f_i$, where $i$ labels the usual $x$, $y$, and $z$ directions. Now, given an exact rotation $\mathbf{R}_e(t)$, we can define the exact rotated frame $e_i(t) := \mathbf{R}_e(t)\, f_i\, \mathbf{R}_e^{-1}(t)$. On the other hand, by integrating the angular velocity, we obtain an approximate frame $a_i(t)$ using any of the methods described in Secs. II, III, and IV. We then define the error norm to be

$$\delta(t) := \sqrt{\sum_i \|e_i(t) - a_i(t)\|^2}, \qquad (25)$$

where the norm of each vector difference is given by the usual inner product.

To integrate the angular velocities, we use standard numerical integration schemes. In particular, since we are most concerned with high-accuracy results and relatively smooth problems, we will use an eighth-order Dormand-Prince method [42, 43] and the Bulirsch-Stoer method [43, 44]. Because our example problems (as well as our motivating example of binary black-hole systems) involve smooth data and the problems are not stiff, these integrators are the best standard general-purpose choices. The Bulirsch-Stoer (B-S) approach is typically capable of taking far fewer steps than the Dormand-Prince (D-P) approach to achieve a given accuracy. However, B-S involves substantially more overhead in each step, and so will frequently take more time than D-P in these examples—even though the latter may typically take ten times as many steps. Nonetheless, we will find generally good behavior with both integrators, showing that general-purpose integrators may typically provide good results with this type of problem.

Both integrators accept as input certain tolerances: a relative tolerance $\text{tol}_{\text{rel}}$ and an absolute tolerance $\text{tol}_{\text{abs}}$. If $y_i$ denotes each of the $N$ evolved variables, and $\delta y_i$ the corresponding estimated error, then the step size of the integrator is adjusted so that

$$\frac{1}{N} \sum_i \frac{\delta y_i^2}{(\text{tol}_{\text{abs}} + |y_i|\, \text{tol}_{\text{rel}})^2}$$

is less than 1. In each of the three approaches to integrating angular velocity we use, the evolved variables represent components of geometric vectors. Those components may oscillate through 0, and error in each of the components should be treated the same—regardless of the instantaneous magnitude of the variable. Thus, we set $\text{tol}_{\text{rel}}$ to 0 in every case, and rely only on $\text{tol}_{\text{abs}}$. It must be noted, however, that this is error tolerance is imposed at each step of the integration. The total instantaneous error $\delta(t)$ will generally grow in time with the number of steps taken.

## B. Precessing and nutating binary

This example emulates the motion of a precessing black-hole binary system. Such binaries are expected to be possible sources for gravitational-wave telescopes [45–48], occurring when one or both black holes have significant spin components that are not aligned with the orbital angular momentum. The full equations that need to be evolved to describe such a system are Einstein's equations, which constitute an enormously complicated system of partial differential equations [49, 50]. No exact closed-form solution of a binary system is known, but inexact solutions can be found using a "post-Newtonian" approximation [51–53], in which the black holes are treated as point sources tracked by their coordinate trajectories. The key variables evolved in this approach are the directions of the spins on the individual black holes, the orbital frequency, and the orientation of the binary.[9] Because the differential equations resulting from the post-Newtonian approximation are still very complicated and—most importantly—coupled, we do not have exact solutions to them. However, we can emulate the characteristics seen in typical precessing evolutions in order to evaluate the best approach to integrating the angular velocity to find the orientation of the binary.

The dominant motion is the orbit, in which the black holes simply rotate about their common center of mass at frequency $\Omega_{\text{orb}}$. We will model this rotation by the rotor $\mathbf{R}_1 = e^{\Omega_{\text{orb}}\, t\, \mathbf{z}/2}$. Exchange of angular momentum between the orbit and the black-hole spins leads to a precession of the orbital axis at frequency $\Omega_{\text{prec}}$, so that the axis roughly traces out a cone of opening angle $\alpha$. However, as angular momentum is radiated in the form of gravitational waves, the orbital angular momentum decreases, which gradually widens this precession cone at some rate $\dot{\alpha}$, which we take to be constant. Tilting the orbital axis down onto this cone can be achieved by the rotor $\mathbf{R}_2 = e^{(\alpha + \dot{\alpha}t)\, \mathbf{x}/2}$, and the precession along this cone can be achieved by rotating *this* rotor by $\mathbf{R}_3 = e^{\Omega_{\text{prec}}\, t\, \mathbf{z}/2}$. Due to off-axis components of the moment-of-inertia tensor, smaller nutations of the orbital axis occur at the orbital frequency on an angular scale $\nu$. The basic tilt can be given by $\mathbf{R}_4 = e^{\nu\, \mathbf{x}/2}$, but this rotor should also be rotated—in this case by $\mathbf{R}_1$. Finally, we also wish to rotate the entire system by some rotor $\mathbf{R}_0$.

The total rotation at any instant is then given by

$$\mathbf{R} = \mathbf{R}_0\, \mathbf{R}_1\, \mathbf{R}_4\, \mathbf{R}_1^{-1}\, \mathbf{R}_3\, \mathbf{R}_2\, \mathbf{R}_3^{-1}\, \mathbf{R}_1. \qquad (26)$$

We choose the constants in these definitions to be comparable to typical values during the last few orbits of a typical comparable-mass binary with strong precession:

$$\Omega_{\text{orb}} = 2\pi/1000, \qquad (27a)$$
$$\Omega_{\text{prec}} = 2\pi/10\,000, \qquad (27b)$$
$$\alpha = \pi/8, \qquad (27c)$$
$$\dot{\alpha} = 2\alpha/100\,000, \qquad (27d)$$
$$\nu = \pi/80, \qquad (27e)$$
$$\mathbf{R}_0 = e^{-3\alpha\, \mathbf{x}/10}. \qquad (27f)$$

--------

[9] The black-hole separation can be calculated from the orbital frequency, and so is not evolved as a separate variable.
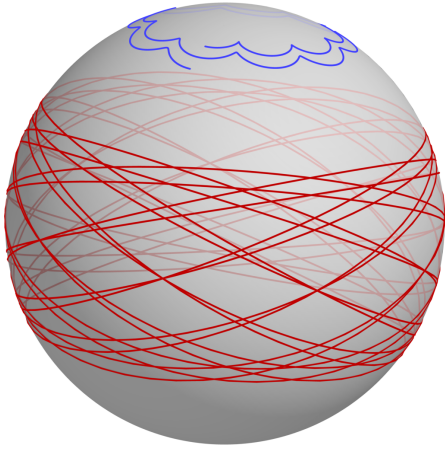
FIG. 1.  **Orbital motion in the precessing and nutating binary**. This figure shows the paths of the unit vectors during the first twenty orbits and two precession cycles (20 000 time units) in the precessing example of Sec. VI B. The blue curve at the top shows the path traced out by the orbital axis (the rotated $z$ vector). The red curve around the center shows the path traced out by the unit separation vector between the two black holes (the rotated $x$ vector). The features seen here include the fast orbital motion, visible in the extensive motion of the red curve; the precession, visible as the broadly circular motion of the blue curve; widening of the precession, visible as the gradually increasing radius of the blue curve; and nutation, visible as the scalloped shape of the blue curve. These are qualitatively the same as features found in real precessing binary black-hole systems, but are approximated here as simple functions so that we have the analytical solution to compare to.

We will evolve this system for a total time of 1 000 000 units,[10] so that the binary goes through 1000 orbits, with 100 precession cycles, and its precession cone opens to three times its original angle. The evolution of a real black-hole binary is obviously much more complicated, but these time scales should provide a more rigorous test of the integration methods than will typically be encountered in simulations of real systems. The orbital motion is depicted in Fig. 1, where all of the features described above can be seen.

Now, since each of the individual rotors $\mathbf{R}_1$ through $\mathbf{R}_4$ is a simple rotation about a constant axis, we can easily differentiate each with respect to time. Furthermore, we can use the product rule to differentiate the product given in Eq. (26) and obtain $\dot{\mathbf{R}}$,

---

[10] All quantities in physical black-hole binaries scale with some power of the total mass of the system $M$. Thus, a binary is generally evolved in arbitrary units; any system with the same mass-ratio and spin parameters is then known in physical units by scaling that result with $M$. For this reason, time is typically measured in units of the "geometrized mass" $G_N M/c^3$, where $G_N$ is Newton's gravitational constant and $c$ is the speed of light. For our example, this means that the unit of time is irrelevant; it could be milliseconds or hours and—in principle—describe a physically possible binary.
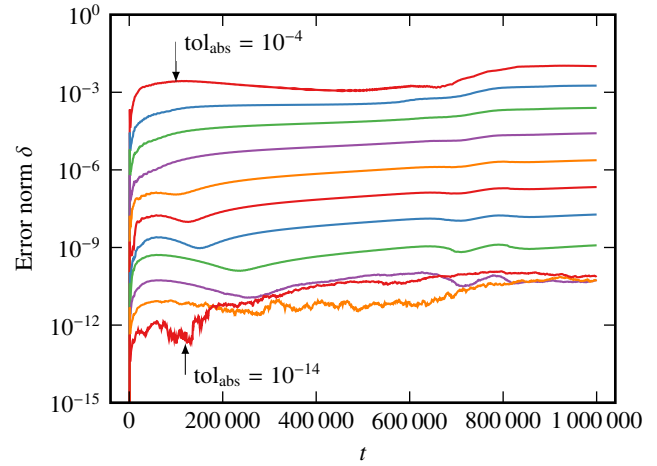


FIG. 2.  **Error norm when integrating using rotors**. This figure shows the error norm $\delta(t)$ given in Eq. (25) for various choices of the absolute tolerance parameter, when integrating the precessing and nutating binary example of Sec. VI B using the rotor approach described in Sec. III with the eighth-order Dormand-Prince integrator. The tolerance is decreased by a factor of 10 for each successive line, demonstrating very clean convergence until the smallest tolerance, which seems to be limited . In the following figures, rather than showing the error as a function of time, we simply select the maximum error on each curve and plot this for various integration methods.

hence also $\boldsymbol{\omega}$. Explicitly, we have

$$\dot{\mathbf{R}}_0 = 0, \tag{28a}$$

$$\dot{\mathbf{R}}_1 = \mathbf{R}_1 \, \Omega_{\text{orb}} \, \mathbf{z}/2, \tag{28b}$$

$$\dot{\mathbf{R}}_2 = \mathbf{R}_2 \, \dot{\alpha} \, \mathbf{x}/2, \tag{28c}$$

$$\dot{\mathbf{R}}_3 = \mathbf{R}_3 \, \Omega_{\text{prec}} \, \mathbf{z}/2, \tag{28d}$$

$$\dot{\mathbf{R}}_4 = 0. \tag{28e}$$

The derivatives of the inverses are found using Eq. (5). We then differentiate Eq. (26) using the product rule to find $\dot{\mathbf{R}}$. Then, plugging the result into Eq. (9), we can determine the angular velocity analytically. We integrate this according to each of the methods detailed above, and finally compare the result of the integration to the original analytical value of Eq. (26).

As a first example, the error norm is shown for a range of tolerances in Fig. 2, using the Dormand-Prince integrator to evolve the rotor. The tolerance is decreased by a factor of 10 for each successive line: $10^{-4}, 10^{-5}, \ldots, 10^{-14}$. We see the resulting error norms also decrease by roughly a factor of 10 each time, indicating good convergence—except for the smallest tolerance. As mentioned above, the tolerance is a local tolerance imposed at each step of the integration, so that over time the actual error should grow to a larger value than the input tolerance, roughly proportional to the number of steps taken. The last two lines take on the noisy appearance characteristic of evolutions limited by machine precision after taking so many steps [54].

Next, we examine the accuracy of the integration using each of the approaches described above, as well as the Bulirsch-Stoer
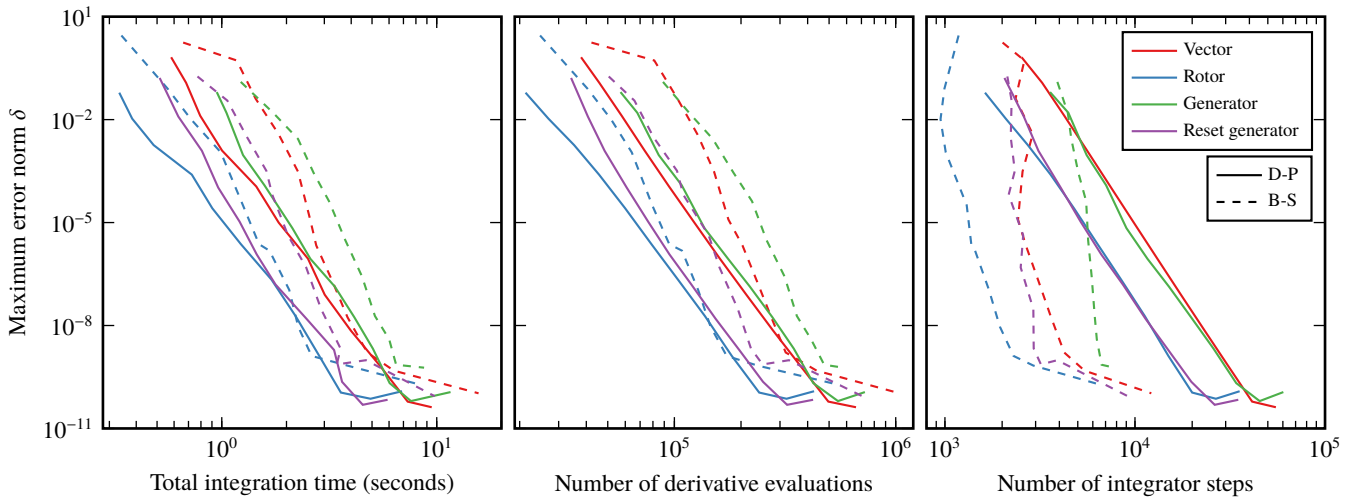
FIG. 3. **Maximum error norm for various integration methods**. This figure shows the maximum value of the error norm $\delta(t)$ defined by Eq. (25), when using the various integration methods and numerical integrators described in the text. The plot on the left shows the error as a function of the total (wall-clock) time taken by the integration; the center plot shows the error as a function of the number of evaluations of the derivative used to achieve that accuracy; and the plot on the right shows the error as a function of the number of steps taken by the integrator. Along each line, different points correspond to different values for the absolute tolerance parameter of the numerical integrator as in Fig. 2—typically resulting in longer integration times and higher accuracy for smaller tolerances. Note that for this example, the eighth-order Dormand-Prince integrator (D-P; solid lines) is usually slightly faster than the Bulirsch-Stoer integrator (B-S; dashed lines), despite the fact that it requires several times as many steps at high accuracy. This is because the B-S integrator involves a very complicated algorithm. In particular, D-P typically requires an average of just over 12 evaluations of the derivatives per step; whereas B-S requires anywhere from 20 to 90, larger numbers being needed for smaller tolerances. It is, however, notable that the B-S integrator achieves nearly its smallest error ($\sim 10^{-9}$) using just over 2000 steps, though the system goes through 1000 orbits during the evolution. These very large steps mean that during a single step the B-S integrator evolves into the more rapidly varying part of the generator integration, even when it is reset between steps, as discussed below.

integrator. Behavior like that seen in Fig. 2 is fairly typical for these cases (as well as other test cases extracted from Refs. [26–28]) but contains somewhat more information than we need. For clarity, the following figures will simply take the maximum error norm for each curve, rather than show the full dependence on time.

Figure 3 shows the maximum error norm during the integration for each of the methods described above, and for each numerical integrator. The plot on the left shows the error versus the total time that integration required. Obviously, the precise timing will depend on the compiler, processor, and various other details,[11] but the relative performance of the methods should be fairly consistent. There are two major factors in the efficiency of any given approach: the numerical integrator, and the representation of the rotation.

For this problem, the Dormand-Prince integrator typically runs somewhat faster than the Bulirsch-Stoer (B-S) integrator, despite the fact that—especially at high accuracies—the B-S integrator can take far fewer steps to achieve the same errors,

as seen in the plot on the right-hand side of Fig. 3. This is unsurprising because the B-S algorithm is very complicated, and each step incurs substantial overhead cost. Its most important feature is that it involves many evaluations of the derivatives [the right-hand sides of Eqs. (1), (10), and (18)], anywhere from 20 for low tolerances to 90 for high tolerances in this example. In fact, a similar plot of the total number of evaluations of the derivatives looks almost exactly like the plot of the total integration time, even for this example where the angular velocity is given by a simple closed-form expression.

The second important feature of these results is the relative efficiency of the different formulations. For a given integrator, the rotor formulation is always more efficient than the vector formulation, which is always more efficient than the simple generator formulation. The latter point—that the generator is the least efficient formulation—may be somewhat surprising considering that it requires only three variables to be integrated, has no constraints that need to be satisfied, and in the simple case of Eq. (11) has a simple linear solution. However, if we reset the generator according to Eq. (20) at the end of each time step if its magnitude is greater than or equal to $\pi/2$, the behavior of the generator solution is much improved, achieving efficiency that essentially the same as that of the rotor approach with the D-P integrator, though somewhere between that of the rotor and vector with the B-S integrator. We can understand these trends by looking at the actual quantities that need to be

---

[11] All computations for this paper were performed on a single core of an Intel Core i7 2.5 GHz processor. Except for the `lsoda` integrator (which is from the `scipy` package, version 0.16.1), all code was written in pure python (version 3.5), much of which was then automatically compiled as needed by the `numba` package (version 0.24), which uses the `LLVM` compiler (version 3.7).
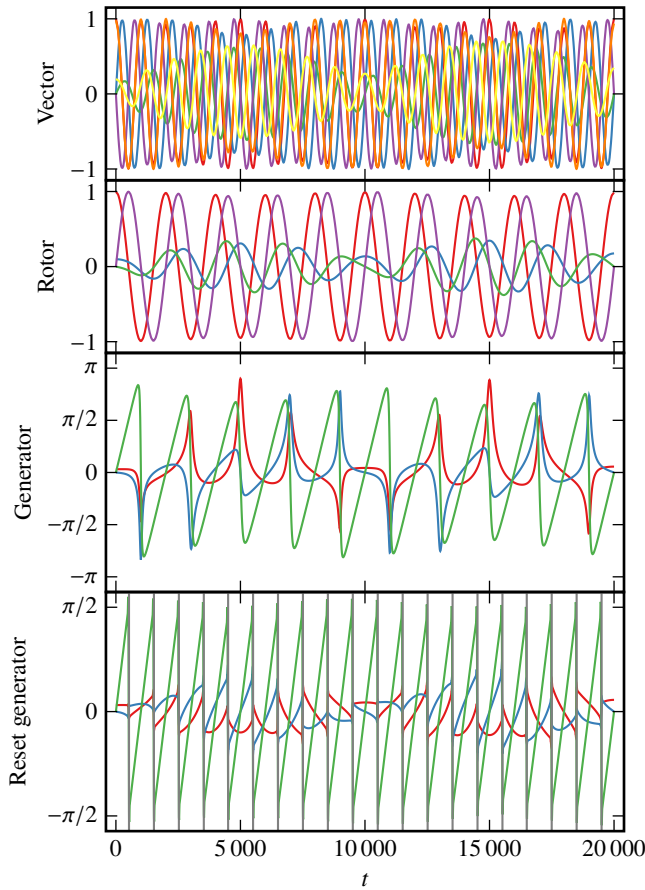
FIG. 4. **Evolved Quantities**. These plots show the actual quantities evolved for the vector, rotor, and generator formulations when solving the precessing example for the first 20 000 time units—one fiftieth of the total time. The identities of the particular components do not matter; only their general behavior is interesting, so we do not label them. The vector components vary twice as rapidly as the rotor components, which is a typical feature of how rotors function, due to the two factors of $\mathbf{R}$ appearing in Eq. (4). This suggests an explanation as to why the integrations of the vectors take roughly twice as long, with twice as many time steps. More surprising is the behavior of the generator. Though we frequently do see roughly linear behavior, each time the amplitude approaches $\pm\pi$, the components change very sharply. This makes the system hard to integrate efficiently. On the other hand, if we discontinuously reset the generator according to Eq. (20), we obtain the components seen in the bottom panel. The integrator does not need to evolve through the discontinuity, and everything in between is smooth and slowly varying, so integration of this quantity is much more efficient.

evolved in each case.

Figure 4 shows the actual quantities evolved in each of the three systems, for the first 20 000 time units. The first point to note is that the six vector components vary twice as quickly as the four rotor components. This is a very general feature of the behavior of rotors, and is due to the two factors of $\mathbf{R}$ found in Eq. (4); in a very rigorous sense, $\mathbf{R}$ is the square-root of the usual rotation operator. Each time the vectors complete one

cycle, the rotor completes only half a cycle. This is related to the spin-1/2 nature of rotors, and the fact that the rotor group [which is isomorphic to SU(2)] forms a double cover of SO(3). The slower dynamics and smaller number of components make it entirely plausible that we should expect the rotor formulation to be roughly twice as fast as the vector formulation in many types of problems. Since time step sizes are affected more directly by the higher derivatives of the integrated functions, it is instructive to look at the second derivative of the rotor:

$$\frac{\mathrm{d}^2\mathbf{R}}{\mathrm{d}t^2} = \frac{1}{2}\dot{\omega}\,\mathbf{R} + \frac{1}{4}\omega^2\,\mathbf{R}. \tag{29}$$

Now, if $2\,|\dot{\omega}| \gtrsim \omega^2$, we can expect the rotor method to require integration steps small enough to resolve the time dependence of $\omega$, which will be faster than that of $\mathbf{R}$. But this will be the same in the vector approach. So in the worst case, we can expect time step sizes to be comparable in the rotor and vector approaches. We might distinguish between vibrations, in which the system oscillates on small angular scales with rapid time dependence, from rotations in which the angular velocity varies relatively slowly. Then the rotor method will lose the factor of 2 advantage in vibrations. In fact we will see two such examples in the Appendix. But even then, fewer equations need to be integrated using rotors, so that there should always be at least a small advantage. Thus, we conclude that the rotor approach will always be preferable to the vector approach.

The generator components vary at roughly the same frequency as the rotor components, and we do indeed see the expected approximately linear behavior for large portions of the evolution. However, these portions are punctuated by very rapid changes in the components. These changes are caused by the system passing close to—but not precisely through—the identity.[12] To resolve these features adequately, the numerical integration must take many small steps around them, leading to the poor behavior seen in Fig. 3. Moreover, the sharp features are highly sensitive to the precise orientation of the system. A slightly different value for $\mathbf{R}_0$ in Eq. (26) leads to very different behavior: much sharper or smoother curves. Whenever the system happens to wander close to the identity, the features will become extremely sharp.

We can discern a pattern in these sharp features: they only occur when the magnitude of the generator becomes large, approaching $\pi$. As discussed near the end of Sec. IV, we can reset the generator to decrease its magnitude whenever it grows beyond $\pi/2$. The reset generator is shown in the bottom panel of Fig. 4. While there are true discontinuities at roughly the orbital period, these are located at discrete times; in between,

---

[12] This is essentially the same as the branch-cut discontinuity familiar from the complex logarithm, which may be "unwrapped" to give a smooth curve. The effect seen here is precisely a three-dimensional version of that discontinuity. In the two-dimensional case, the system is topologically forced to return to the identity. In three dimensions there is no such requirement, so the system will more typically just miss $\pm\pi$, and the logarithm cannot be made smoother by unwrapping.

the components of the generator are very smooth. We can apply this to numerical integration by simply imposing the reset at the end of each step the integrator takes. The discontinuities do not need to be resolved in any way by the integrator, so that they do not affect the size of the time steps it can take. Thus, by applying this reset, the generator approach goes from being the slowest one seen here to being competitive with the rotor approach. One interesting effect of this is that the B-S integrator can take so few steps, and hence such large steps, that from beginning to end of the step the system may go well past the point where it could have been reset. That is, within a single step the system will evolve to a very dynamical state. And since the generator can only reasonably be reset *between* steps, this diminishes the performance of the B-S integrator when applied to the generator approach, which is why we see the rotor approach being substantially more efficient.

Not shown are the results for the constraint-damped system where $f_0$ is evolved by Eq. (2), and $f_1$ is evolved by Eq. (3). Whenever the damping parameters $\lambda$ and $\mu$ are large enough to noticeably impact the results, this system is orders of magnitude slower than any other system because it is stiff. For good measure, a third numerical integrator was also used for this system: the lsoda integrator as implemented in the scipy package [55], which is designed for stiff systems. While that does slightly improve the efficiency over the D-P and B-S integrators for most values of $tol_{abs}$, it still cannot compete with the efficiency of the non-damped vector system. There may exist applications for which such damping could be effective—perhaps when lower-order integration is used with noisy data. But given the results of this example, it seems likely that the rotor or generator approaches would be more effective in every case.

## VII. CONCLUSIONS

This paper has presented three fundamental methods of integrating angular velocity, along with various possible improvements. These methods were then evaluated by application to a rigorous test case with an analytically known solution. The results show that even standard integration algorithms can deliver very accurate evolutions with great efficiency.

The direct evolution of vectors by Eq. (1) is elementary, and is equivalent to evolution of the rotation matrix at the most naive level. We can eliminate half of the redundancy in this approach by evolving two basis vector, and computing the third as the unique perpendicular unit vector completing a right-handed triple. In our test case, we saw that this method approaches the best method within a factor of 2 in efficiency. But this factor of 2 is likely to be a very general feature, due to the nature of quaternion and generator representations of rotations, whenever the angular velocity itself varies more slowly than the vectors it describes. This essentially make the vector twice as dynamic as the quaternion and generator, requiring twice as many time steps during integration. Two constraint-damping terms were suggested in Eqs. (2) and (3), as a way to possibly improve the accuracy of integration at a given time-step size,

or equivalently allow the integrator to take larger steps. It turns out that these terms simply make the system stiff, leaving it orders of magnitude less efficient than the other approaches. Generally, it seems clear that direct integration of the vectors will not be the preferred method for any system.

A better alternative is integration of the rotor responsible for the rotation, by Eq. (10). This rotor is a nonzero quaternion which acts on any vector according to Eq. (4), resulting in the rotated version of that vector. As discussed in Sec. III, the unusual use of the inverse in Eq. (4) frees us from the usual normalization constraint on the quaternion; Eq. (10) is always the correct evolution equation, regardless of the normalization of the quaternion. This allows the quaternion to provide the most efficient method of integration found in this paper, despite the fact that the quaternion uses four degrees of freedom to represent a rotation that has only three intrinsic degrees of freedom. In a way, that fourth degree of freedom is hidden.

The final method we examined was direct evolution of the generator of the rotation by Eq. (18). Using quaternion techniques it is a simple matter to relate a rotation to its generator, with no need for intermediate translations to matrices or other representations. This explicitly requires just three degrees of freedom, and simplistic arguments suggest that the components of the generator should behave in a simple—nearly linear—manner. It turns out that such arguments are overly simplistic, and the components actually undergo very rapid evolution during certain stages of a typical rotation, as seen in the third panel of Fig. 4. However, it is possible to discontinuously change these components after certain time steps, reducing the magnitude of the generator, and making the evolution much simpler. With this improvement, integration by generator goes from being the least efficient of these three methods to very closely rivaling the rotor method.

Because of these additional complications (and perhaps the transcendental function in its evolution equation), the generator method cannot generally be expected to be as robustly efficient as the rotor method, though different situations may provide a minor advantage to one or the other. If the system is restricted to very small rotations—staying in the neighborhood of the identity—the discontinuities will never come into play and the generator method may be very slightly more efficient than the rotor method. This may be the case in twisting of beams, for example, where a complete rotation of the beam from its original position may be uncommon. However, for larger rotations, the rotor method will frequently be able to achieve a given accuracy with fewer steps because the rotors never enter the delicate region for which the generator reset was introduced. Taken together, these considerations suggest that the rotor approach should be a good general choice unless specific features of the problem recommend the generator.

Nonetheless, the differences between the rotor and generator methods are fairly slight. Section V describes generalizations of the generator method to other Lie groups. In particular, it suggests a method for finding exact evolution equations in many cases—as opposed to resorting to finite truncations as in the Magnus and Munthe-Kaas algorithms. Such a

method finds possible application in integrating relativistic motions in the Lorentz group $SO^+(3,1)$, or even the conformal spacetime representation $Spin(4,2)$ which can incorporate translations [31]. These topics, of course, are beyond the scope of this paper.

A final conclusion may also be drawn from these results. Quite simply, the general-purpose numerical integrators used here are capable of evolving rotations very accurately and stably when used with an adequate formalism. The example of the precessing black-hole binary is rigorous, involving both large rotations due to the basic orbital nature of the system, as well as smaller precessional and nutational oscillations on very different timescales. Nonetheless, over many multiples of these dynamical timescales, the integrators are able to achieve high accuracy, approaching the limits of machine precision.

### ACKNOWLEDGMENTS

### Appendix: Additional numerical examples

For the sake of additional and more direct comparisons to other references, this appendix briefly presents several more numerical examples. Zupan and Saje [26] constructed four examples by inventing analytic functions to be taken as the components of the rotation vector $\boldsymbol{\vartheta}(t)$, which is essentially the generator of the rotation. In the language of quaternions this is just twice the logarithm, so $\mathbf{r} = \boldsymbol{\vartheta}/2$. Now, because the expressions for $\boldsymbol{\vartheta}$ are given as simple functions of time, we can also find the derivative as $\dot{\mathbf{r}} = \dot{\boldsymbol{\vartheta}}/2$. Thus, we can obtain analytic expressions for the angular velocity $\omega$ using Eq. (17). We can then integrate the angular velocity to deduce the frame, and compare that result to the analytic result of directly using the rotation operator $\mathbf{R} = e^{\mathbf{r}}$.

Plots of the maximum error norm versus the number of steps taken by the integrator are shown in Fig. 5 for each of the Zupan-Saje examples. The exact generators are listed in the respective titles. The upper right and lower left, in particular, show examples of systems that might be called vibrational; their angular velocities vary quickly relatively to the frames they describe. In particular, both systems satisfy $2|\dot{\omega}| \gg \omega^2$, especially the system shown in the lower left. As discussed below Eq. (29), this means that the numerical integrators must track the evolution of $\omega$, which means that the rotor method does not have such a large advantage over the vector method. Nonetheless, the rotor approach is slightly more efficient even in these cases.

It must be noted that the approach used to devise these numerical examples is highly synthetic, and can lead to very unrealistic motions. In particular, the unbounded growth of the generator in the final example (lower right plot) exhibits extremely large and variable rotations, yet returns precisely to the identity rotation many times with increasing frequency. In fact, the naive implementation of the generator method breaks down entirely with this example, as the equations become stiff. The reset generator method shown here, however, is actually the most efficient one in that case, precisely because it is well suited to this type of rotation. With the notable exception of that one line, we generally obtain roughly the same behavior seen in the example of Sec. VI B: the rotor and generator methods being comparable, and the vector method being substantially less efficient. Moreover, comparison to the results found by Zupan and Saje [26] shows that the high-order general-purpose integrators used here provide far more accurate results. Note that more recent work [27, 28] by those authors and collaborators obtained improved precision using highly specialized integrators.

[1] B. P. Abbott *et al.*, Phys. Rev. Lett. **116** (2016), 10.1103/PhysRevLett.116.061102.

[2] O. J. Woodman, *An introduction to inertial navigation*, Technical Report UCAM-CL-TR-696 (University of Cambridge, Computer Laboratory, 2007).

[3] R. B. Miller, Journal of Guidance, Control, and Dynamics **6**, 287 (1983).

[4] L. P. Candy, *Kinematics in conformal geometric algebra with applications in strapdown inertial navigation.*, Ph.D. thesis, University of Cambridge, Great Britain (2012).

[5] D. Wu and Z. Wang, Advances in Applied Clifford Algebras **22**, 1151 (2012).

[6] J. C. Simo, Computer Methods in Applied Mechanics and Engineering **49**, 55 (1985).

[7] F. A. McRobie and J. Lasenby, International Journal for Numerical Methods in Engineering **45**, 377 (1999).

[8] M. B. Ignagni, Journal of Guidance, Control, and Dynamics **13**, 363 (1990).

[9] M. B. Ignagni, Journal of Guidance, Control, and Dynamics **13**, 0576b (1990).

[10] M. B. Ignagni, Journal of Guidance, Control, and Dynamics **19**, 424 (1996).

[11] W. Magnus, Communications on Pure and Applied Mathematics **7**, 649 (1954).

[12] E. Hairer, G. Wanner, and C. Lubich, *Geometric Numerical Integration: Structure-Preserving Algorithms for Ordinary Differential Equations*, 2nd ed. (Springer, New York, 2006).

[13] H. Munthe-Kaas, Applied Numerical Mathematics Proceedings of the NSF/CBMS Regional Conference on Numerical Analysis of Hamiltonian Differential Equations, **29**, 115 (1999).

[14] P. E. Crouch and R. Grossman, Journal of Nonlinear Science **3**, 1 (1993).
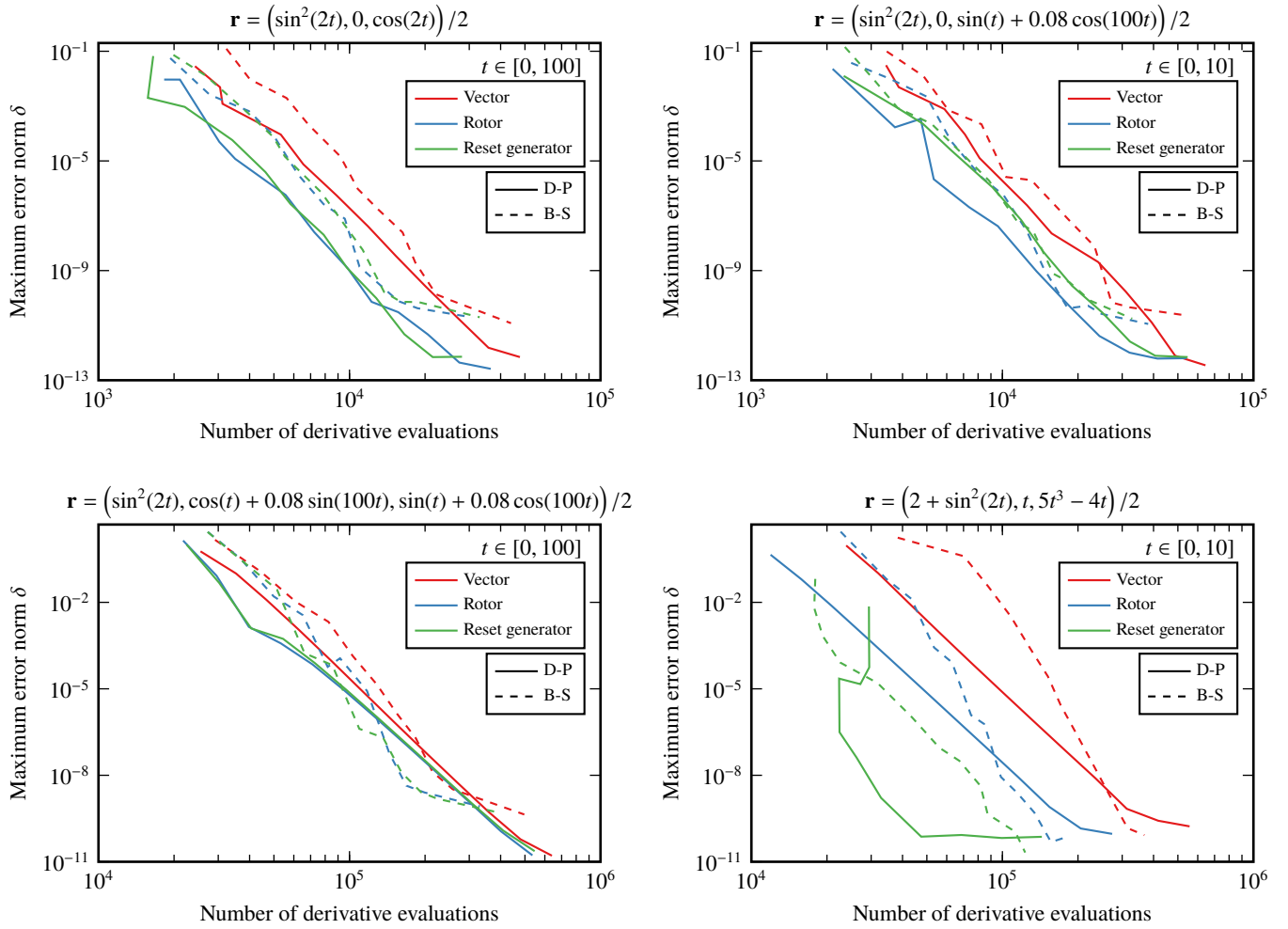
FIG. 5. **Numerical examples of Zupan-Saje**. These plots show the same quantities as in the center plot of Fig. 3, except that each system is one of the four examples of Zupan and Saje [26]. The exact generators are shown in the title of each plot, which are integrated over the range of times shown above the legends. The data give the error of the integrated angular velocity for values of $\mathrm{tol}_{\mathrm{abs}}$ ranging from $10^{-4}$ to $10^{-14}$.

[15] C. L. Bottasso and M. Borri, Computer Methods in Applied Mechanics and Engineering **164**, 307 (1998).

[16] J. C. Simo and K. K. Wong, International Journal for Numerical Methods in Engineering **31**, 19 (1991).

[17] X. Lin and T. Ng, International Journal for Numerical and Analytical Methods in Geomechanics **19**, 653 (1995).

[18] O. R. Walton and R. L. Braun, in *Flow of Particulates and Fluids: Proceedings, Joint DOE/NSF Workshop on Flow of Particulates and Fluids, Ithaca, New York, Sept. 29–Oct. 1, 1993*, edited by S. I. Plasynski, W. C. Peters, and M. C. Roco (National Technical Information Service, 1993).

[19] A. Munjiza, J. P. Latham, and N. W. M. John, International Journal for Numerical Methods in Engineering **56**, 35 (2003).

[20] G. Bogfjellmo and H. Marthinsen, "High order symplectic partitioned Lie group methods," (2013), arXiv:1303.5654 [gr-qc].

[21] R. Shivarama and E. P. Fahrenthold, Journal of Dynamic Systems, Measurement, and Control **126**, 124 (2004).

[22] C. Kane, J. E. Marsden, M. Ortiz, and M. West, International Journal for Numerical Methods in Engineering **49**, 1295 (2000).

[23] A. Lew, J. E. Marsden, M. Ortiz, and M. West, International

[24] L. Candy and J. Lasenby, in *Guide to Geometric Algebra in Practice*, edited by L. Dorst and J. Lasenby (Springer London, 2011) pp. 105–125.

[25] S. M. Johnson, J. R. Williams, and B. K. Cook, International Journal for Numerical Methods in Engineering **74**, 1303 (2008).

[26] E. Zupan and M. Saje, Advances in Engineering Software **42**, 723 (2011).

[27] E. Zupan and D. Zupan, Mechanics Research Communications **55**, 77 (2014).

[28] A. Treven and M. Saje, Advances in Engineering Software **85**, 26 (2015).

[29] M. J. Crowe, *A history of vector analysis: The evolution of the idea of a vectorial system* (Dover, New York, 1985).

[30] D. Hestenes and G. Sobczyk, *Clifford algebra to geometric calculus* (Kluwer Academic Publishers, Norwell, MA, 1987).

[31] C. Doran and A. Lasenby, *Geometric algebra for physicists*, 4th ed. (Cambridge Univ. Press, 2010).

[32] T. G. Vold, Am. J. Phys. **61**, 491 (1993).

[33] W. K. Clifford, American Journal of Mathematics **1**, 350 (1878).

[34] D. Hestenes, Celestial mechanics **30**, 151 (1983).

Journal for Numerical Methods in Engineering **60**, 153 (2004).

[35] A. Hatcher, *Algebraic Topology*, 1st ed. (Cambridge University Press, New York, NY, 2001).

[36] M. Boyle, Phys. Rev. D **87**, 104006 (2013).

[37] F. S. Grassia, J. Graph. Tools **3**, 29 (1998).

[38] J. J. Duistermaat and J. A. C. Kolk, *Lie groups* (Springer, 2000). See Sec. 1.5.

[39] W. Miller, *Symmetry Groups and Their Applications*, Pure and Applied Mathematics (Academic Press, New York, 1972) see Lemma 5.3.

[40] B. Hall, *Lie Groups, Lie Algebras, and Representations*, Graduate Texts in Mathematics No. 222 (Springer International Publishing, 2015).

[41] C. Doran, D. Hestenes, F. Sommen, and N. V. Acker, J. Math. Phys. **34**, 3642 (1993).

[42] E. Hairer, G. Wanner, and S. P. Nørsett, *Solving Ordinary Differential Equations I: Nonstiff Problems*, Springer Series in Computational Mathematics, Vol. 8 (Springer Berlin Heidelberg, Berlin, 1993).

[43] W. H. Press, S. A. Teukolsky, W. T. Vetterling, and B. P. Flannery, *Numerical Recipes 3rd Edition: The Art of Scientific Computing*, 3rd ed. (Cambridge University Press, New York, NY, 2007).

[44] J. Stoer and R. Bulirsch, *Introduction to Numerical Analysis*, Texts in Applied Mathematics No. 12 (Springer New York, 2002).

[45] V. Kalogera, ApJ **541**, 319 (2000).

[46] R. O'Shaughnessy, J. Kaplan, V. Kalogera, and K. Belczynski, Astrophys. J. **632**, 1035 (2005).

[47] P. Grandclément, M. Ihm, V. Kalogera, and K. Belczynski, Phys. Rev. D **69**, 102002 (2004).

[48] L. S. Collaboration and V. Collaboration, Class. Quantum Gravity **27**, 173001 (2010).

[49] R. M. Wald, *General relativity*, 1st ed. (Univ. of Chicago Press, 1984).

[50] C. W. Misner, K. S. Thorne, and J. A. Wheeler, *Gravitation*, 1st ed. (W. H. Freeman, 1973).

[51] L. Blanchet, Living Rev. Relativ. **9** (2006).

[52] A. Buonanno, Y. Chen, and M. Vallisneri, Phys. Rev. D **67**, 104025 (2003).

[53] M. Boyle, L. E. Kidder, S. Ossokine, and H. P. Pfeiffer, "Gravitational-wave modes from precessing black-hole binaries," (2014), arXiv:1409.4431 [gr-qc].

[54] M. Boyle, L. Lindblom, H. P. Pfeiffer, M. A. Scheel, and L. E. Kidder, Phys. Rev. D **75**, 024006 (2007).

[55] E. Jones, T. Oliphant, P. Peterson, *et al.*, "SciPy: Open source scientific tools for Python," (2001–), [Online; accessed 2016-03-11].